Article ID: 1006-8775(2021) 01-0081-06

Rapid−Scan and Polarimetric Phased−Array Radar Observations of a Tornado in the Pearl River Estuary

ZHANG Yu (张 羽)[1], BAI Lan-qiang (白兰强)[2, 3], MENG Zhi-yong (孟智勇)[4], CHEN Bing-hong (陈炳洪)[1], TIAN Cong-cong (田聪聪)[1], FU Pei-ling (傅佩玲)[1]

(1. Guangzhou Meteorological Observatory, China Meteorological Administration, Guangzhou 511430 China;
2. School of Atmospheric Sciences/ Guangdong Province Key Laboratory for Climate Change and Natural Disaster Studies, Sun Yat-sen University, Zhuhai, Guangdong 519082 China;
3. Southern Marine Science and Engineering Guangdong Laboratory (Zhuhai), Zhuhai, Guangdong 519082 China;
4. Department of Atmospheric and Oceanic Sciences, School of Physics, Peking University, Beijing 100871 China)

Abstract: The strong destructive winds during tornadoes can greatly threaten human life and destroy property. The increasing availability of visual and remote observations, especially by Doppler weather radars, is of great value in understanding tornado formation and issuing warnings to the public. In this study, we present the first documented tornado over water detected by a state-of-the-art dual-polarization phased-array radar (dual-PAR) in China. In contrast to new-generation weather radars, the dual-PAR shows great advantages in tornado detection for its high spatial resolution, reliable polarimetric variables, and rapid-scan strategy. The polarimetric signature of copolar cross-correlation coefficient with anomalously low magnitude appears to be effective for verifying a tornado and thus is helpful for issuing tornado warnings. The Guangdong Meteorological Service has been developing an experimental X-band dual-PAR network in the Pearl River Delta with the goal of deploying at least 40 advanced dual-PARs and other dual-polarization weather radars before 2035. This network is the first quasi-operational X-band dual-PAR network with unprecedented high coverage in the globe. With such high-performance close-range PARs, efficient operational nowcasting and warning services for small-scale, rapidly evolving, and damaging weather (e.g., tornadoes, localized heavy rainfall, microbursts, and hail) can be expected.

Key words: tornado; waterspout; phased-array radar; dual-polarization; China
CLC number: P406 **Document code:** A
https://doi.org/10.46267/j.1006-8775.2021.008

1 INTRODUCTION

Tornadoes are violently rotating columns of air, in contact with thunderstorms and the ground, which are destructive to life and property. The growth in availability of visual and remote observations, especially by Doppler radars, is of great value to the understanding of their formation and the issue of warnings to the public. Doppler weather radars are one of the most efficient modern systems for weather state surveillance and short-term forecast and warning. Currently, China has deployed a nationwide radar network composed of more than 200 S- and C-band weather radars, i. e., the China New Generation Doppler Weather Radar (CINRAD) network [1-3]. Although these new-generation weather radars have achieved great success in severe weather forecast and warning [4-7], it is often hard for them to observe small-scale weather systems like tornadoes, i.e., systems with scales of O (100) m, limited by their sparse spatial resolution and scanning time interval.

In recent years, dual-polarization phased-array radars (dual-PARs) have demonstrated a significant potential for detecting tornadoes efficiently due to its agile electronic beam steering capability [8]. They showcase great advantages in tornado detection with a high spatial resolution, high accuracy measurement of polarimetric variables, and rapid scan strategy. Among dual-PAR and new-generation radar observations, the rapid-scan PAR proved most advantageous in depicting tornadic storm-scale processes such as the rapid changes of mesocyclone intensity, storm organization, and inflow magnitude [9,10]. Such PARs with fast update speed were demonstrated to potentially increase the lead time of tornado warning [11]. Also owing to the high-temporal-frequency sampling capability, the rapid-scan PAR would benefit storm-scale modeling by data assimilation, which may prolong the lead time of severe weather warning [12].

To precisely monitor tornadoes, a higher-

Received 2020-09-21; **Revised** 2020-11-15; **Accepted** 2021-02-15

Founding: Key-Area R & D Program of Guangdong Province (2020B1111200001); National Key R & D Program of China (2017YFC1501701); National Natural Science Foundation of China (41875051); Guangzhou Municipal Science and Technology Planning Project (201903010101)

Biography: ZHANG Yu, Senior Engineer, primarily undertaking research on weather radar data processing and application.

Corresponding author: BAI Lan-qiang, e-mail: bailq@mail.sysu.edu.cn

performance observation system is required, especially in developed city agglomerations such as the Pearl River Delta (PRD) that are vulnerable to destructive weather [13,14]. The PRD is a tornado-prone region in China and is highly populated with busy river ports [15-17]. A damaging tornado is a significant threat to the lives and marine traffic in this area. In addition to tornadoes, other small-scale weather systems such as microbursts are also hard to observe by new-generation operational radars. Due to such an urgent need, a quasi-operational (experimental) network of dual-PARs has been being established in the PRD since 2017. By 2020, the Guangdong Meteorological Administration has deployed a 17 dual-PAR network in the PRD, providing unprecedentedly high sampling resolution below 3 km altitude over the city agglomerations. The early validation experiments on thunderstorms, heavy rainfall and hail have suggested that this dual-PAR network generates reliable remotely sensed data [18]. This network will consist of a total of 40 advanced X-band dual-PARs by 2035. As the first quasi-operational X-band dual-PAR network with unprecedented high coverage in the globe, the network will facilitate operational forecasting and warning services on small-scale, rapidly evolving, and destructive weather including tornadoes, downbursts, hail, and local heavy rainfall.

This study presents a successfully observed tornado by the newly established PRD dual-PAR network. To our best knowledge, this is the first dual-PAR detected waterspout (i.e., tornado over water) in China that is documented in scientific literature. The rest of this paper is organized as follows. Section 2 describes the radar data used in this study. The observational analysis is presented in section 3. This manuscript is summarized in section 4.

2 DATA DESCRIPTION

The mosaics of radar reflectivity obtained from operational weather radars were utilized to characterize the morphology of convective systems. The radar data used in this study were collected by two polarimetric radars. The PAR deployed in Nansha District, Guangzhou was located approximately 6 km to the south of the reported tornado that will be discussed in this study (Fig. 1). The other radar was an operational S-band CINRAD that was deployed in Panyu District, Guangzhou (CINRAD-GZ), which was located approximately 30 km to the northwest of the tornado. During this event, the PAR operated electronically scanned X-band planar antenna with dual polarization and used 12 elevation angles (0.9°, 2.7°, 4.5°, 6.3°, 8.1°, 9.9°, 11.7°, 13.5°, 15.3°, 17.1°, 18.9°, and 20.7°) in a 360° volumetric update time of about 90 s. The radial gate spacing was 30 m and the azimuthal interval was 0.9° . The CINRAD-GZ operated in volume coverage pattern 21 (VCP21), scanning nine elevation angles (0.5°, 1.5°, 2.4°, 3.3°, 4.3°, 6°, 9.9°, 14.6° , and 19.5°) with a volumetric update time of nearly 360 s. The data of this radar were collected in 250-m range bins approximately every 1° in azimuth. During this event, the dual-PAR had a wider beam width (horizontal 3.6°, vertical 1.8°) than the CINRAD-GZ (~1° in the horizontal and vertical). The lowest levels of the PAR and CINRAD-GZ were approximately 420 and 490 m above the ground level (AGL) at the tornado location, respectively. Following the self-consistent method suggested by Park et al.

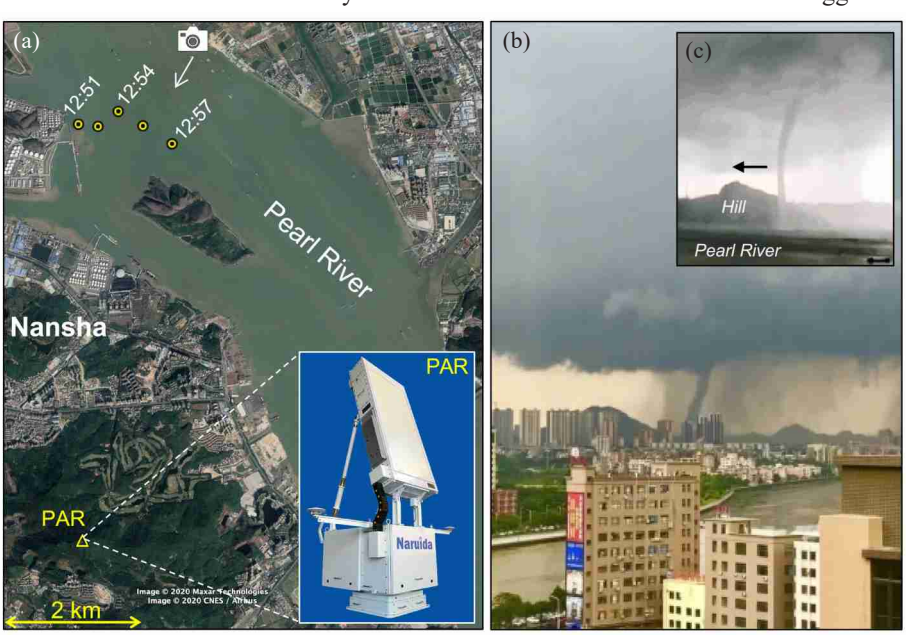

Figure 1. (a) Locations of the tornadic vortex signatures (TVSs; yellow dots) observed by the phased-array radar (PAR; triangle) in Nansha District, Guangzhou from 12:51 to 12:57 LST on 1 June 2020. The PAR device is shown at the bottom-right corner. (b) Photo of the condensation funnel collected from media. (c) Condensation funnel snapshot taken in the direction as denoted by the white arrow in (a). The black arrow represents the moving direction of the tornado.

(2005) [19], the corrections of reflectivity (Z_H) and differential reflectivity (Z_{DR}) attenuation were conducted based on the specific differential phase K_{DP}.

3 RESULTS

The reported tornado occurred from approximately 12: 51 to 12: 57 local standard time (LST) on 1 June 2020 over the water of the Pearl River Estuary (Fig. 1a). It formed at the southern end of a meridionally oriented linear mesoscale convective system (referred to as the arrow in Fig. 2a). The tornado was spawned by a weak supercell. Before the tornadogenesis, a clear "hook" echo signature (tornado often occurs nearby) was observed on a scale of 2 km (Fig. 3a). The subsequent tornado was located within the weak-echo hole at the tip of the hook echo at low levels (e.g., Figs. 3c and 4a, b). Due to the relatively coarse sampling resolution, the CINRAD-GZ was hard to observe the fine structure and rapid evolution of the supercell. For example, the PAR well captured the weak-echo hole below 2.3 km AGL, while the CINRAD-GZ appeared to totally miss the signature even at the lowest level (Fig. 3d).

Owing to its super-high spatiotemporal resolution, the PAR successfully captured the tornado vortex signatures [TVSs [20]; Doppler velocity signature of a tornado or of an incipient tornado-like circulation aloft] (Figs. 2b, c). The maximum gate-to-gate azimuthal radial velocity difference was 22 m s^{-1} directly over the tornadic circulation at 420 m AGL. As shown in Figs. 2b and c, the cyclonic Doppler couplets (indicative of the tornado circulation) are generally 500 m in diameter. Although the CINRAD-GZ also detected the TVS, the detailed structures are missing (Fig. 2d). Apparently, the sampling resolution of the new-generation weather radar is not high enough to depict the fine structures and storm-scale processes of the tornado and also its parent supercell during this event. Accurate tornado detection and warning will save lives, and support emergency management and disaster mitigation. The rapid-scan PAR with high spatial resolution in detecting tornadoes give us confidence in future tornado forecast and warning. It is worth noting that the tornado position on the ground cannot be accurately identified because the tornado occurred over the river (Fig. 1c). Considering that the condensation funnel maintained in relatively vertical shape and the lowest sampling level was only ~400 m AGL, we used the centroid of the lowest-level TVS as the proxy of tornado position in this study.

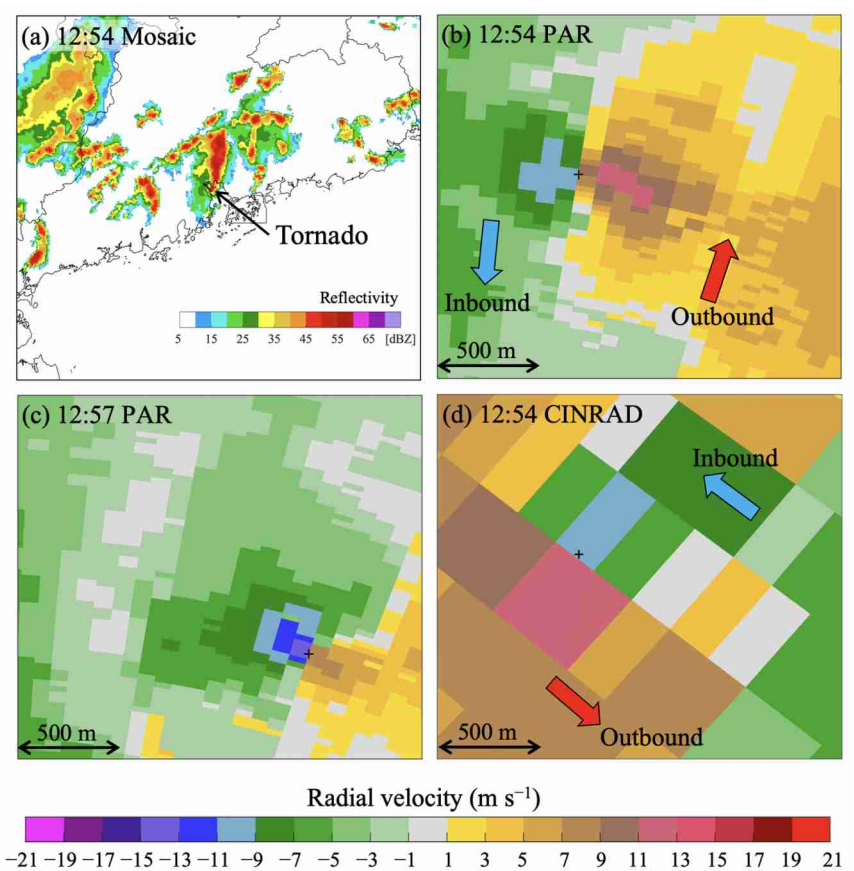

Figure 2. (a) Snapshot of the mosaic of radar reflectivity (units: dBZ) in south China obtained from National Meteorological Center. (b), and (c) Radial velocity (units: m s^{-1}) at the 0.9° elevation angle of the dual-PAR showing the tornadic vortex. The tornado location (black cross) and the inbound (blue arrow) and outbound (red arrow) directions are also shown for reference. (d) Same as (b) but for the 0.5° radial velocity of the CINRAD-GZ.

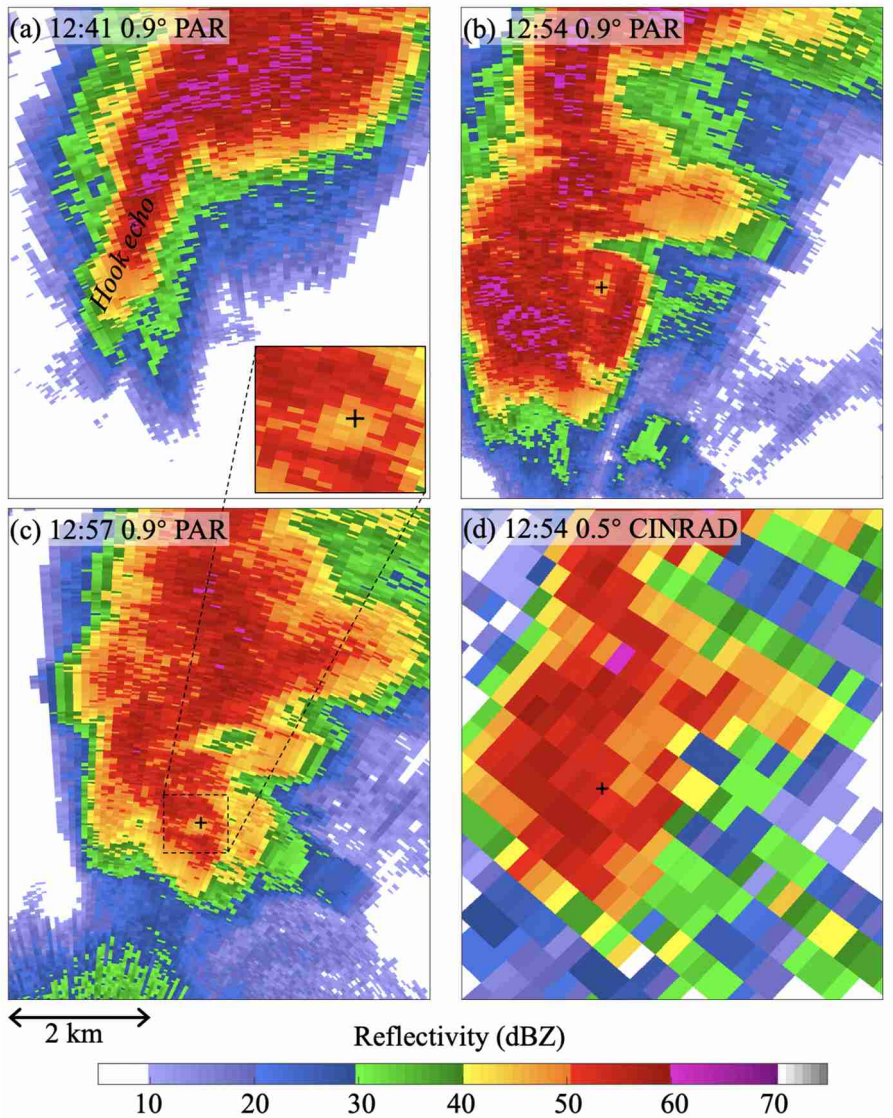

Figure 3. (a)-(c) Reflectivity (units: dBZ) at the 0.9° elevation angle of the dual-PAR showing the evolution of the tornadic supercell around the hook echo region. The "hook" echo signature is labeled in (a) for reference. The weak-echo hole around the tornado (black cross) in (c) is enlarged in the bottom-right corner in (a). (d) Same as (c) but for the 0.5° reflectivity of the CINRAD-GZ. For the four panels, the distance scale is presented at the bottom-left.

In addition to the super-high resolution, the polarimetric variables obtained from the PAR are also helpful for tornado detection [21,22]. For example, anomalously low copolar cross-correlation coefficient (ρ_{HV}) and Z_{DR} were located right at the tornado location (Fig. 4c-g). The ρ_{HV} is often associated with lofted tornadic debris which typically has random orientation and irregular shape and thus results in a low ρ_{HV} signature. Because the present tornado was located over the water surface and thus tended to carry little debris, the low ρ_{HV} signature may be primarily a result of the diversity of water-drop sizes, orientations and shapes induced by the strong shear in the tornadic circulation zone [23,24]. As shown in Figs. 4c, d, the tornado zone is characterized by Z_{DR} close to 0 dB, suggesting randomly oriented scatters in that region. The polarimetric variable ρ_{HV} is usually effectively used for verifying a tornado, especially when the tornado is not visually observed, and thus aids in the subsequent tornado warning. During this event, low ρ_{HV} signatures were observable collocating with the TVSs (referred to as the crosses in Figs. 2 and 4g) at the lowest level of the dual-PAR, while they were not observed by the CINRAD-GZ (not shown). Because the PRD region will have densely deployed dual-PARs, polarimetric tornado signatures tend to be detected at a relatively close range with high probability in the future, and would thus be helpful in potentially extending the tornado-warning lead time.

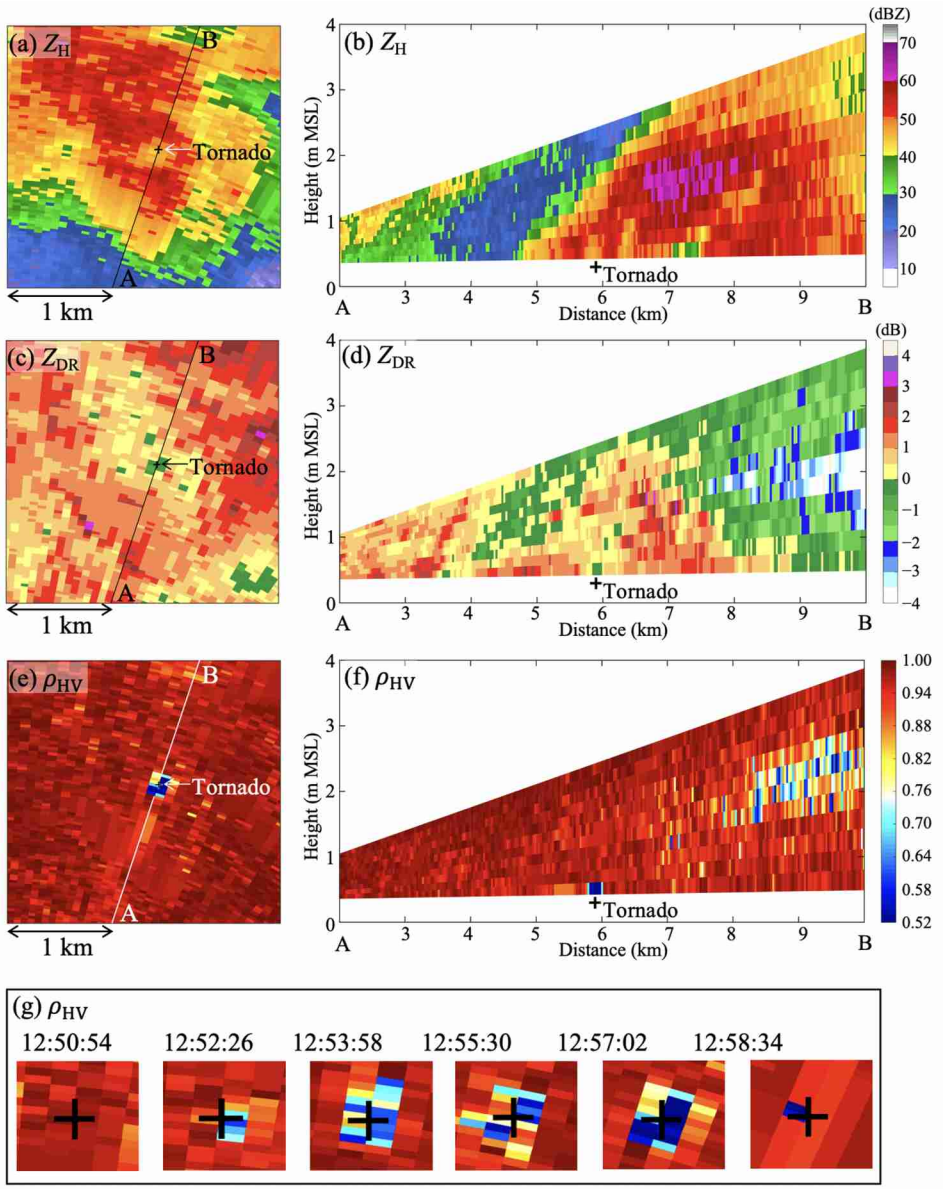

Figure 4. (a) Reflectivity (Z_H, units: dBZ), (d) differential reflectivity (Z_{DR}, units: dB) and (e) copolar cross-correlation coefficient (ρ_{HV}) at the 0.9° elevation angle around the tornado location (crosses marked by arrow) at 12:57:02 LST on 1 June 2020. Vertical cross sections of (b) Z_H, (d) Z_{DR} and (d) ρ_{HV} along the line AB as shown in (a), (c) and (e), respectively. The tornado location is marked by the black cross below the lowest radar level. (g) Copolar cross-correlation coefficient enlarged around the tornado locations (crosses) at different time.

4 SUMMARY

This paper presents the first documented tornado detected by a dual-PAR network in China. The tornado formed on the water at the mouth of the Pearl River with a duration of approximately 7 min. The low-level tornadic vortex was relatively weak and small in diameter in contrast to the midlatitude violent tornadoes. Although the tornadic vortex was small and short-lived, the dual-PAR was still able to detect it effectively owing to the super-high spatiotemporal resolution. In agreement with previous studies, the polarimetric signature of the copolar cross-correlation coefficient is powerful for tornado detection and verification. In conclusion, the future of tornado detection and warning in China seems to be bright, relying on the high-performance dual-PAR observing system. The establishment of a dual-PAR network is of fundamental importance for both the weather service and tornado research communities. The high-resolution data with high-accuracy measurement of polarimetric variables may help us better understand the internal physical processes and microphysical information of destructive tornadoes and their parent storms. The documented tornado in this paper may be a "milestone" of the dual-PAR-based tornado detection and warning system for large city agglomerations in China in the near future.

Acknowledgments: The authors thank Dr. ZHENG Yong-guang and Dr. YU Xiao-ding for their constructive comments on the early version of the manuscript. The authors would also like to thank the two anonymous reviewers for their valuable suggestions.

REFERENCES

[1] ZHAO K, HUANG H, WANG M, et al. Recent progress in dual-polarization radar research and applications in China [J]. Adv Atmos Sci, 2019, 36(9): 961-974, https://doi.org/10.1007/s00376-019-9057-2.

[2] WU C, LIU L, LIU X, et al. Advances in Chinese dual-polarization and phased-array weather radars: Observational analysis of a supercell in southern China [J]. J Atmos Oceanic Technol, 2018, 35(9): 1785-1806, https://doi.org/10.1175/JTECH-D-17-0078.1.

[3] BAI L, CHEN G, HUANG L. Image processing of radar mosaics for the climatology of convection initiation in south China [J]. J Appl Meteorol Climatol, 2020, 59(1): 65-81, https://doi.org/10.1175/JAMC-D-19-0081.1.

[4] BAI L, CHEN G, HUANG L. Convection initiation in monsoon coastal areas (south China) [J]. Geophys Res Lett, 2020, 47(11): e2020GL087035, https://doi. org / 10.1029/2020GL087035.

[5] MENG Z, YAO D, BAI L, et al. Wind estimation around the shipwreck of Oriental Star based on field damage surveys and radar observations [J]. Sci Bull, 2016, 61(4): 330-337, https://doi.org/10.1007/s11434-016-1005-2.

[6] MENG Z, BAI L, ZHANG M, et al. The deadliest tornado (EF4) in the past 40 years in China [J]. Wea Forecasting, 2018, 33(3): 693-713, https://doi.org/10.1175/WAF-D-17-0085.1.

[7] LUO Y, QIAN W, GONG Y, et al. Ground-based radar reflectivity mosaic of mei-yu precipitation systems over the Yangtze River-Huaihe River basins [J]. Adv Atmos Sci, 2016, 33(11): 1285-1296, https://doi.org/10.1007/s00376-016-6022-1.

[8] FRENCH M M, BLUESTEIN H B, POPSTEFANIJA I, et al. Mobile, phased-array, Doppler radar observations of tornadoes at X band [J]. Mon Wea Rev, 2014, 142(3): 1010-1036, https://doi.org/10.1175/MWR-D-13-00101.1.

[9] HEINSELMAN P, LADUE D, KINGFIELD D M, et al. Tornado warning decisions using phased-array radar data [J]. Wea Forecasting, 2015, 30(1): 57-78, https://doi.org/10.1175/WAF-D-14-00042.1.

[10] KUSTER C M, HEINSELMAN P L, AUSTIN M. 31 May 2013 El Reno tornadoes: Advantages of rapid-scan phased-array radar data from a warning forecaster's perspective [J]. Wea Forecasting, 2015, 30(4): 933-956, https://doi.org/10.1175/WAF-D-14-00142.1.

[11] WILSON K A, HEINSELMAN P L, KUSTER C M, et al. Forecaster performance and workload: Does radar update time matter? [J]. Wea Forecasting, 2017, 32(1): 253-274, https://doi.org/10.1175/WAF-D-16-0157.1.

[12] SUPINIE T A, YUSSOUF N, JUNG Y, et al. Comparison of the analyses and forecasts of a tornadic supercell storm from assimilating phased-array radar and WSR-88D observations [J]. Wea Forecasting, 2017, 32(4): 1379-1401, https://doi.org/10.1175/WAF-D-16-0159.1.

[13] YU X, ZHENG Y. Advances in severe convection research and operation in China [J]. J Meteorol Res, 2020, 34(2): 189-217, https://doi.org/10.1007/s13351-020-9875-2.

[14] HUANG X, YU X, YAN L, et al. An analysis on tornadoes in Typhoon Ewiniar [J]. Acta Meteorol Sin, 2019, 77(4): 645-661.

[15] BAI L, MENG Z, SUEKI K, et al. Climatology of tropical cyclone tornadoes in China from 2006 to 2018 [J]. Sci China Earth Sci, 2020, 63(1): 37-51, https://doi. org / 10.1007/s11430-019-9391-1.

[16] CHEN J Y, CAI X H, WANG H Y, et al. Tornado climatology of China [J]. International J Climatol, 2018, 38(5): 2478-2489, https://doi.org/10.1002/joc.5369.

[17] FAN W J, YU X D. Characteristics of spatial-temporal distribution of tornadoes in China [J]. Meteorol Mon, 2015, 41: 793-805 (in Chinese).

[18] CHENG Y, FU P, HU D, et al. The Guangzhou phased-array radar networking scheme [J]. Meteorol Mon, 2020, 46: 823-836 (in Chinese).

[19] PARK S, BRINGI V N, CHANDRASEKAR V, et al. Correction of radar reflectivity and differential reflectivity for rain attenuation at X band, Part I: Theoretical and empirical basis [J]. J Atmos Oceanic Technol, 2005, 22 (11): 1621-1632, https://doi.org/10.1175/JTECH1803.1.

[20] BURGESS D W, LEMON L R, BROWN R A. Tornado characteristics revealed by Doppler radar [J]. Geophys Res Lett, 1975, 2(5): 183-184, https://doi. org / 10.1029 / GL002i005p00183.

[21] KUMJIAN M R, RYZHKOV A V. Polarimetric signatures in supercell thunderstorms [J]. J Appl Meteorol Climatol, 2008, 47(7): 1940-1961, https://doi. org / 10.1175 / 2007JAMC1874.1.

[22] RYZHKOV A, SCHUUR T J, BURGESS D W, et al. Polarimetric tornado detection [J]. J Appl Meteorol Climatol, 2005, 44(5): 557-570, https://doi.org/10.1175/JAM2235.1.

[23] KUMJIAN M R, RYZHKOV A V, MELNIKOV V M, et al. Rapid-scan super-resolution observations of a cyclic supercell with a dual-polarization WSR-88D [J]. Mon Wea Rev, 2010, 138(10): 3762-3786, https://doi. org / 10.1175/2010MWR3322.1.

[24] Van Den BROEKE M S, Van Den BROEKE C A. Polarimetric radar observations from a waterspout-producing thunderstorm [J]. Wea Forecasting, 2015, 30 (2): 329-348, https://doi.org/10.1175/WAF-D-14-00114.1.

Citation: ZHANG Yu, BAI Lan-qiang, MENG Zhi-yong, et al. Rapid-scan and polarimetric phased-array radar observations of a tornado in Pearl River Estuary [J]. J Trop Meteor, 2021, 27(1): 81-86, https://doi.org/10.46267/j.1006-8775.2021.008.